Routine Regional Moment Tensor Inversion for Earthquakes in the Greek Region: The National Observatory of Athens (NOA) Database (2001–2006)

K. I. Konstantinou,[1] N. S. Melis,[2] and K. Boukouras[2]

Online material: Solution quality classification criteria and moment tensor solution data.

INTRODUCTION

The routine use of regional broadband data for the determination of moment tensors of even very small events ($Mw \sim$ 3.5) has considerably enhanced our understanding of tectonic processes in many active regions worldwide (*e.g.*, Kao and Jian 2001; Braunmiller *et al.* 2002; Kubo *et al.* 2002; Pondrelli *et al.* 2002; Clinton *et al.* 2006; Risteau 2008). This development can be attributed to a number of reasons, such as the ability to generate accurate synthetic seismograms for a given velocity model and an increase in the amount and quality of data at regional distances. An additional reason may also be the variety of available methods for regional moment tensor inversion that utilize different parts of the recorded waveform, like surface waves (Thio and Kanamori 1995), body and surface waves (Zhao and Helmberger 1993), or just the long-period part of the signal (Ritsema and Lay 1995).

Greece has high seismicity, and large events in the past have caused significant damage and casualties (for an overview see Papazachos and Papazachou 1997). Thus, a systematic study of source properties can help seismic hazard mitigation efforts and offer insights into the seismogenic patterns of the Greek region. Most available source mechanisms of previous events in Greece were derived either from *P*-wave polarities (Papazachos *et al.* 1983, 1988; Papadopoulos *et al.* 1986) or from the inversion of teleseismic waveforms recorded by the Global Seismic Network (Lyon-Caen *et al.* 1988; Hatzfeld *et al.* 1996; Bernard *et al.* 1997; Kiratzi and Louvari 2003; Benetatos *et al.* 2004). However, the former approach depends heavily on station coverage and the reliability of the first-motion readings, while
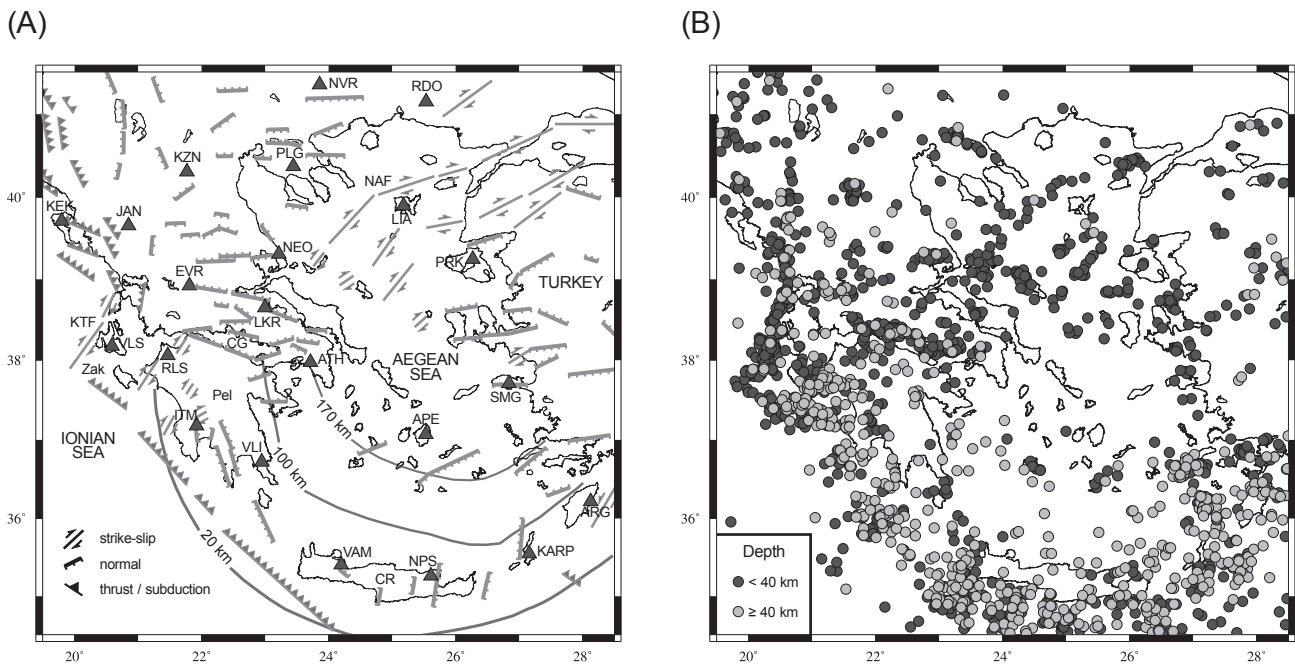
the latter one can be used only for moderate to large events ($Mw > 5.0$).

Since 1997 the National Observatory of Athens (NOA), Institute of Geodynamics, has begun upgrading its nationwide seismic network. This involved the upgrade of existing stations from analog to digital and the installation of a number of new stations. Since early 2001 (when most of the stations became fully operational) high-quality recordings of numerous events have already accumulated. In several cases NOA data have been used to derive regional moment tensors, such as for the 26 July 2001 ($Mw = 6.4$) Skyros earthquake (Melis *et al.* 2001), the 2 December 2002 ($Mw = 5.7$) Vartholomio earthquake (Roumelioti *et al.* 2004), and the 14 August 2003 ($Mw = 6.3$) Lefkada earthquake (Benetatos *et al.* 2005). More recently, this nationwide network has been merged with three regional networks operated by Greek universities, thus increasing the number of available stations and the volume of recorded data (for examples of studies using data from this new unified network see Evangelidis *et al.* 2008 or Konstantinou, Melis, *et al.* 2009).

In this work we report on the routine determination of moment tensor solutions of events occurring in the Greek region for the period 2001–2006 and covering a broad magnitude range ($Mw \sim 3.6$–6.7). We start by giving background information about the tectonic setting and past seismicity followed by a description of available data and inversion methodology. Specific examples of moment tensor inversion results are presented that highlight the main data characteristics and performance of the method. We then perform a simple statistical analysis of this moment tensor database and compare our solutions with those reported by other agencies for the Greek region in terms of moment magnitude and focal mechanism compatibility. Finally, we close with conclusions about the implementation of routine moment tensor inversions in the Greek region.

1. Institute of Geophysics, National Central University, Jhongli, Taiwan
2. Institute of Geodynamics, National Observatory of Athens, Greece

▲ **Figure 1.** A) Map showing the main tectonic features in Greece and surrounding regions, after Papazachos and Papazachou (1997). The curves for 20, 100, and 170 km are isodepth curves showing the hypocentral depth distribution of earthquakes occurring along the Wadati-Benioff zone (from Papazachos *et al.* 2000). The triangles represent seismic stations operated by NOA during the period of this study (2001–2006). Zak: Zakynthos island, Pel: Peloponnese, CG: Corinth Gulf, CR: Crete, NAF: North Anatolian fault, KTF: Kefalonia transform fault. B) Map of well-determined locations of earthquakes that have occurred in Greece and surrounding regions during the period 1964–2005. The locations were taken from the global relocation catalog of Engdahl *et al.* (1998) and its subsequent updates.

TECTONIC SETTING AND SEISMICITY

The Greek region is characterized by complicated tectonics as a result of the operation of three different processes (Figure 1A). In the southern Aegean, the African lithosphere is subducting beneath the Eurasian plate at a rate of 0.9 cm/yr (McClusky *et al.* 2000). Because of the subduction a Wadati-Benioff zone is developed that extends down to 180 km as evidenced by the hypocentral distribution of intermediate depth events (Papazachos *et al.* 2000). In the west, the subduction terminates south of Zakynthos island, and in the rest of the Ionian islands (as well as northwest Greece and Albania) collisional processes dominate. Collision is induced by the anti-clockwise movement of the Apulian against the Eurasian plate, and the Kefalonia transform fault (KTF) serves as a boundary between subduction in the south and collision in the north (Baker *et al.* 1997; Sachpazi *et al.* 2000). In the central and northern Aegean different branches of the right lateral north Anatolian fault (NAF) traverse the area as a result of the westward motion of the Anatolian plate that has started since the late Miocene (Le Pichon and Angelier 1979; Le Pichon *et al.* 1995). Extensional deformation prevails everywhere else, even though the direction of the extension may vary from N-S in mainland Greece to E-W in southern Peloponnese and western Crete (Hollenstein *et al.* 2008).

Figure 1B shows the epicenters of earthquakes in the Greek region for the period 1964–2005 as relocated by Engdahl *et al.* (1998) using travel times compiled by the International Seismological Centre (ISC). It can be clearly seen that much of the shallow seismicity (< 40 km) is focused along the KTF in the Ionian islands, along the NAF branches in the northern Aegean, and across the Corinth Gulf. Several destructive earthquakes have occurred in these areas in the past, and present-day microseismicity is also quite high. Significant seismicity related to the bending and subduction of the African plate is also observed to the south of Peloponnese and Crete. Most of the intermediate depth events in the southern Aegean are fairly small, but some can be large enough to cause damage and casualties, as was the case with the 8 January 2006 (*Mw* 6.7) Kythira earthquake (Konstantinou *et al.* 2006; Konstantinou, Lee et. al 2009). From this description it is evident that a sizable database of moment tensor solutions would greatly help the study of regional tectonics and geodynamic processes.

DATA AND METHODOLOGY

During the interval of this study the Hellenic Seismological Broadband Network (HL) operated by NOA consisted of 22 stations equipped with three-component seismometers recording in a continuous mode (Figure 1A and also see the dedicated Web page http://bbnet.gein.noa.gr for the current status of the network). Most of the sensors were Lennartz Le-3D; a few were Guralp CMG-40T, recording periods of up to 20 and 30 s respectively. Signals were transmitted through leased telephone lines to the NOA headquarters in Athens where events were processed by NOA staff. This involved manual picking of *P* and

S phases and location using HYPO71 (Lee and Lahr 1972). Local magnitude reported at NOA bulletin was estimated during the period of our study by using the analog recordings of a Wood-Anderson seismometer that was installed in 1964 at the same location with World-Wide Standard Seismograph Network (WWSSN) station ATH and utilizing the attenuation function of Richter (1935) (hereafter this magnitude will be denoted as M_{LATH}). Since early 2004 an automatic processing procedure was implemented where automatic picking of *P* phases and location of the epicenter of each event was performed by assuming a fixed hypocentral depth of 10 km. Local magnitude was also estimated automatically using synthetic Wood-Anderson traces and following the methodology of Hutton and Boore (1987) (hereafter this magnitude will be denoted as M_{LAUT}). More details about the network's components and its routine operation can be found in Melis and Konstantinou (2006). Events that were recorded in at least three stations with a signal-to-noise ratio of 3 or larger were considered as potential candidates for moment tensor inversion.

Moment tensor inversions are usually performed in the frequency band 0.05–0.02 Hz for small earthquakes and in the band 0.05–0.01 Hz for large events. The limited bandwidth of our instruments means that inversions should be performed in a relatively narrow range of frequencies with 0.05 Hz being the lower cutoff frequency. Daily quality control of the recorded waveforms at each station (available at http://bbnet.gein.noa.gr/QC/htdocs/index.html) indicated that the band 0.05–0.08 Hz was least susceptible to long-period noise at the majority of the stations, and it could be used for moment tensor inversion. This represents a compromise between instrument limitations and the need to include long periods in the inversion so as to limit the influence of the assumed velocity model on the inversion results. For our routine inversions we use a number of velocity models that cover different parts of the Greek region. Specifically, we use the results of Karagianni *et al.* (2005) to model waveforms with ray paths that traverse the northern/southern Aegean. For ray paths traversing the Peloponnese we use the model suggested by Novotny *et al.* (2001), while for western Greece we use the velocity model derived by Haslinger *et al.* (1999). In areas where intermediate-depth events occur (southern Aegean and Peloponnese), upper mantle velocities of the corresponding models have been constrained using the mantle tomography results of Papazachos and Nolet (1997).
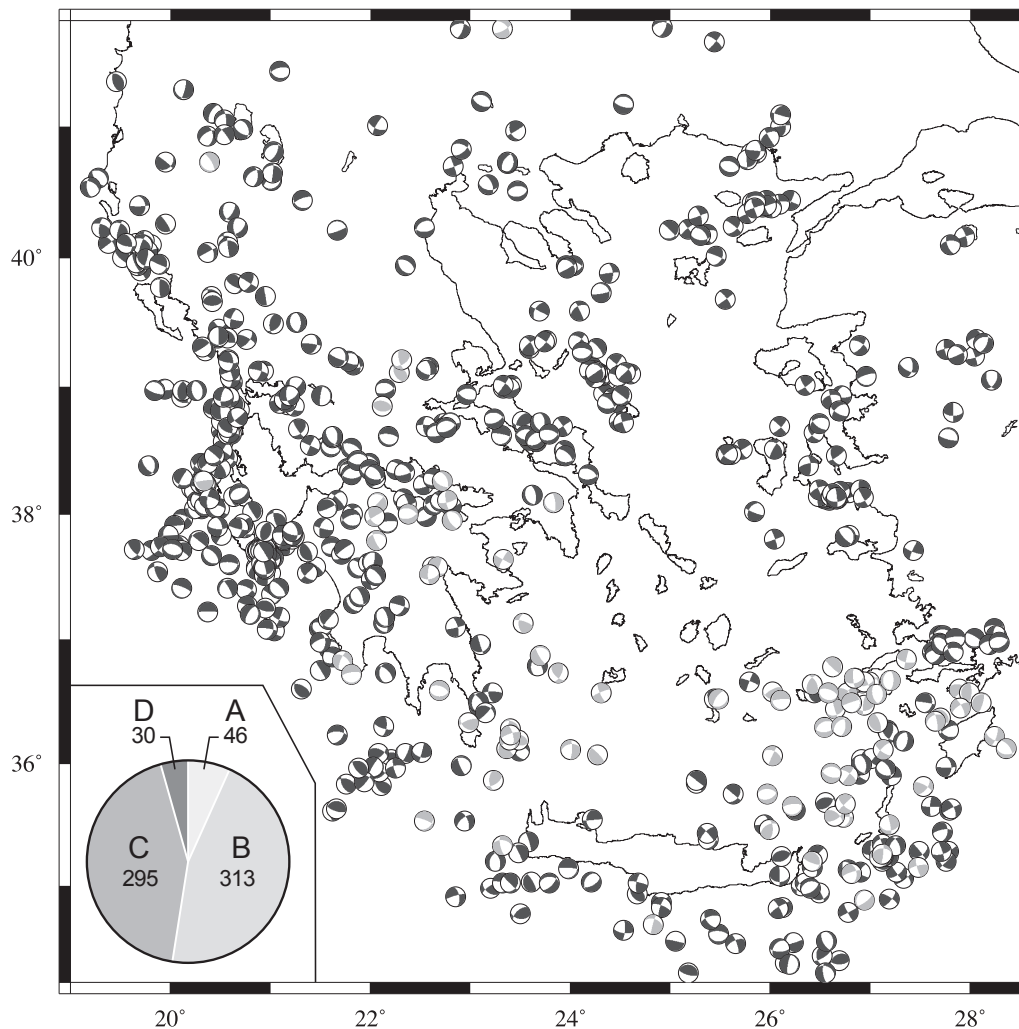
A linear, time-domain moment tensor inversion method with a point source approximation is applied to the three-component waveforms of each event. The method uses the long-period part of the signal to invert for the deviatoric part of the moment tensor and is fully described in a number of publications, most notably Randall *et al.* (1995), Ghose *et al.* (1998), and Stich *et al.* (2003). We usually included in the inversion at least three stations that covered different azimuths on the focal sphere and with an epicentral distance not exceeding 250 km. We calculated Green's functions for different depths using the reflectivity method of Kennett (1983) as implemented by Randall (1994), using the epicenter location provided by the manual analysis and assuming a delta source time function for small events. For moderate to large events the Green's functions were convolved with a trapezoid of appropriate length prior to the inversion. Data preparation included the reduction of waveforms to displacement and rotation of horizontal components to radial and transverse with respect to the event's epicenter. Both the observed waveforms and Green's functions were filtered between 0.05–0.08 Hz using a two-pole Butterworth filter and aligned according to their arrival times in order to minimize the effects of the assumed velocity structure and any source mislocation. Test inversions showed that inverting waveforms longer than 60 s resulted in much higher misfits, since our simple velocity models cannot predict complicated waveforms at the 0.05–0.08 Hz frequency band in which we are working. Therefore in all our inversions we use a fixed waveform length of 60 s, which is three times the maximum period of our observations (20 s).

Initial inversions were performed at a coarse depth interval of 5 km followed by a finer one every 1–2 km around the depth that exhibited the lowest misfit (for intermediate-depth events these values become 10 and 5 km, respectively). We evaluate the quality of moment tensor solutions by jointly considering the average misfit and compensated linear vector dipole (CLVD) amount that is a measure of the non-double-couple part of the solution. Therefore each solution has a quality code that consists of a letter (A–D) based on the misfit value and a number (1–4) according to the CLVD amount (Table S1 in the electronic supplement). In cases where a solution was derived using only two stations, or the station coverage is not optimal, we add to the quality code a minus (–) sign. In this way we successfully inverted moment tensor solutions of 684 events in Greece and surrounding regions, of which 359 solutions (~ 52%) are of quality B or higher (Figure 2). Table S2 in the electronic supplement summarizes the location, moment tensor inversion results, and quality of each solution. At this point it should be noted that the depth of minimum misfit/CLVD derived from our inversions is comparable to the hypocentral depth estimated by the inversion of arrival times, and a comparison of these two depth values will be presented later.

EXAMPLES OF INVERSION RESULTS

In this section we present some example events that have been inverted using the methodology outlined previously. Through these examples we aim to highlight characteristics of the inversion results that are also representative of the other solutions contained in our database. Several other agencies publish moment tensor solutions for events in the Greek (also European-Mediterranean) region, most notably the Global CMT group (GCMT, former Harvard CMT), SED (Swiss Seismological Service, routine inversions performed at ETH Zurich) and the Regional CMT group (RCMT, routine inversions performed at the Italian Instituto Nazionale di Geofisica e Vulcanologia [INGV]). Whenever available we compare our solutions to the others in the following examples, while a more detailed comparison will be given in a later section for all common events.

▲ **Figure 2.** Map of the 684 moment tensor solutions that are included in our database (2001–2006). Black beach balls represent events with focal depths less than 40 km while gray beach balls show those with focal depths equal to or larger than 40 km. The inset at the lower left corner shows the quality partition of solutions contained in the database (for definition of the letter code A–D see Table S1 in the electronic supplement).
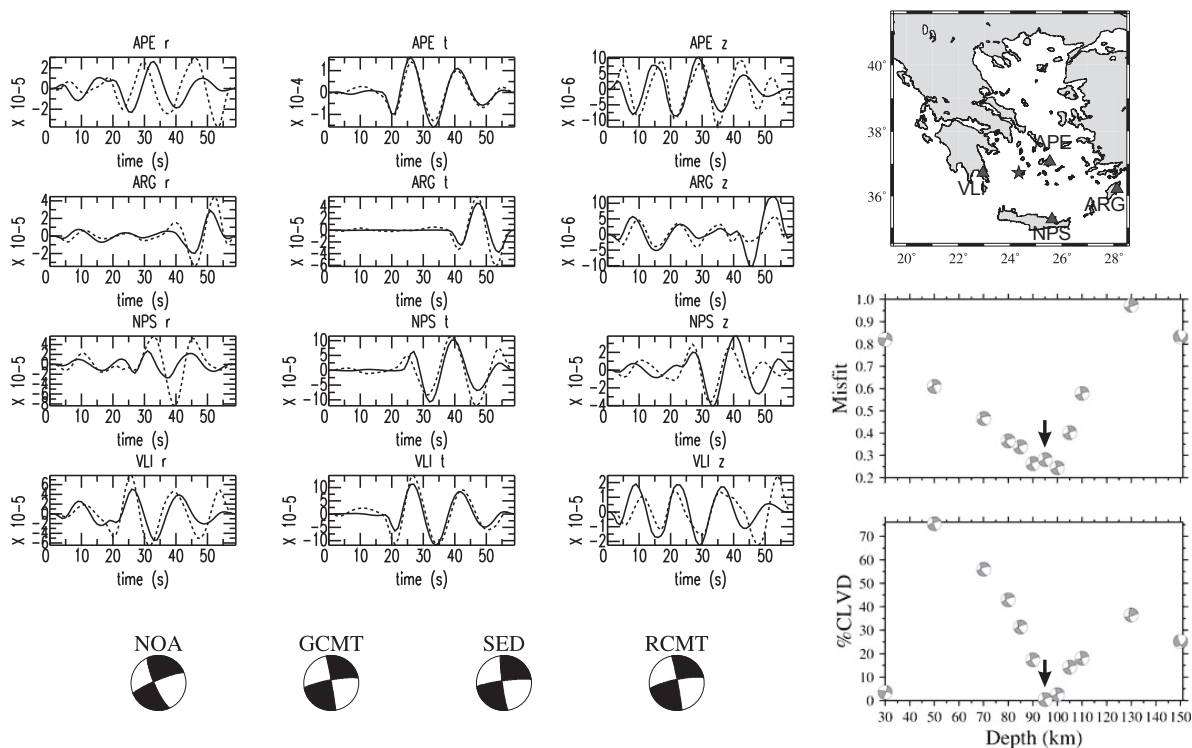
21 May 2002 20:53:30 (GMT)

This intermediate-depth event was located in the southern Aegean near Milos island at a hypocentral depth of 97 km and had magnitude M_{LATH} = 5.1 as listed in the NOA catalog. The location of the event in the middle of the network provides an excellent azimuthal coverage, and we invert waveforms recorded at four stations (Figure 3). The misfit versus depth curve has a minimum between 90–100 km while the CLVD versus depth exhibits a sharp minimum at 95 km, which is also selected as the solution depth for this event. A purely strike-slip focal mechanism is determined by our analysis that is very similar to the GCMT, SED, and RCMT solutions. The moment magnitude derived from the inversion is equal to 5.8, which is far larger than the calculated local magnitude. This large difference highlights the difficulties encountered in the estimation of M_{LATH} when large earthquakes occur near the Athens station (ATH). In these cases, the analog Wood-Anderson record becomes saturated and the calculated magnitude is likely to be underestimated by more than 0.5 units.
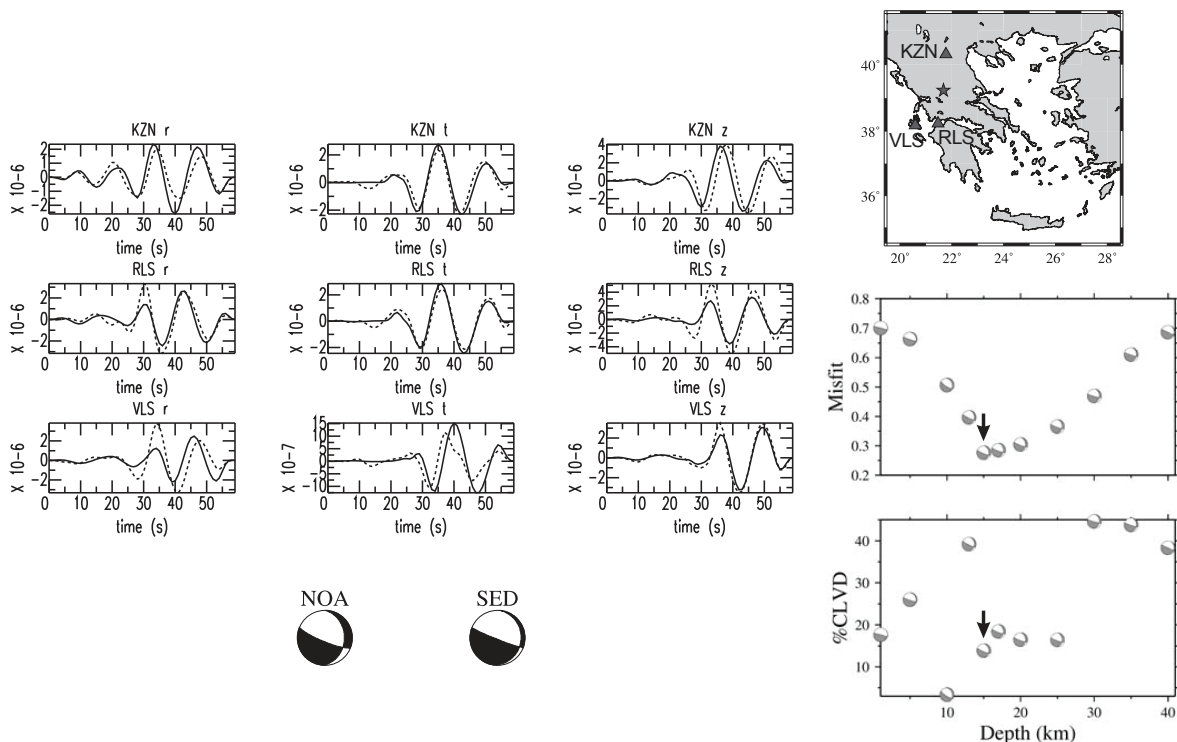
11 December 2004 21:03:19

This event has been located in the Greek mainland at a depth of 15 km and has M_{LATH} = 4.2 and M_{LAUT} = 4.1 respectively. Again the azimuthal coverage is quite good and allows us to select three stations for inversion that lie at completely different azimuths (Figure 4). The misfit versus depth curve has a clear minimum at 15 km while the CLVD versus depth curve has a local minimum at the same depth. The location's depth inferred from our inversion coincides with the location's hypocentral depth. The moment magnitude of this event is equal to 4.3, which is very close to M_{LATH}. Due to the small magnitude of the event only SED has calculated a moment tensor solution, which exhibits normal faulting with a small strike-slip component. As can be seen, this solution is very similar to the one determined by our inversion.
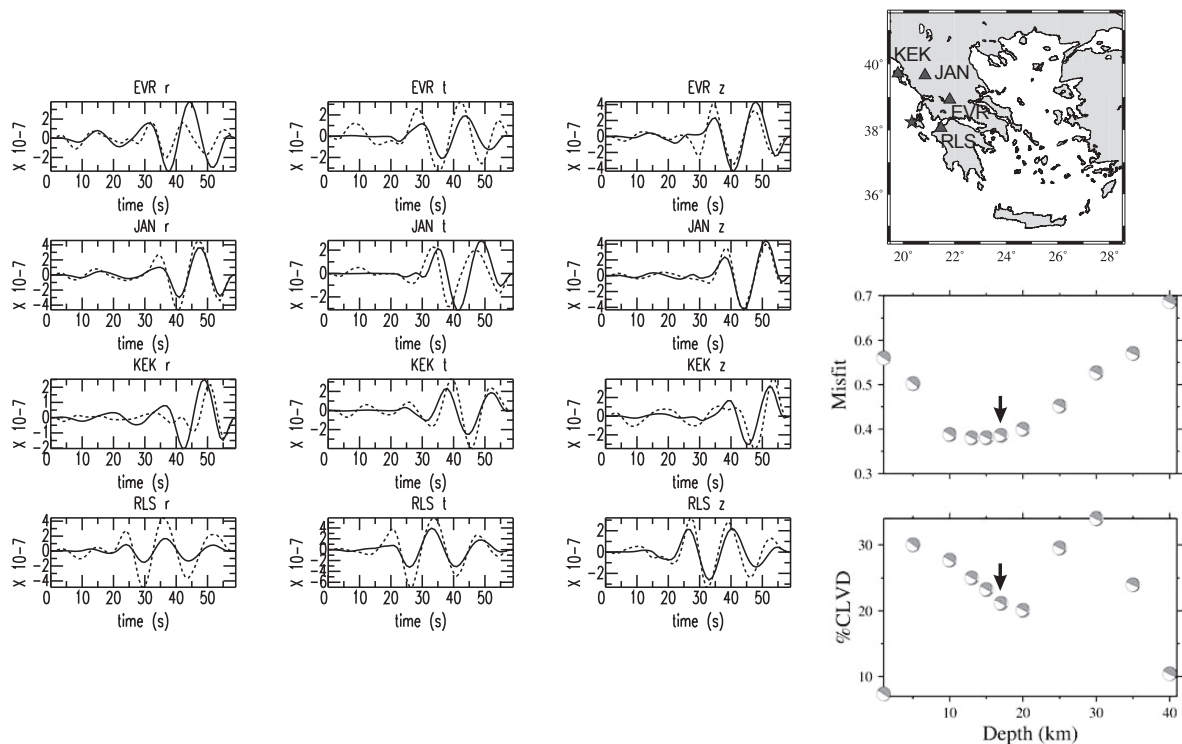
26 August 2005 23:16:51

Here we want to give an example of an event that is one of the smallest that we have modeled and also lies at the edge of our

▲ **Figure 3.** Moment tensor inversion results for an event that occurred on 21 May 2002 in the southern Aegean. The star on the map represents the epicenter of the earthquake as located by NOA and the triangles indicate the stations that were used in the inversion. The selected solution is highlighted with an arrow in the misfit/CLVD-versus-depth diagrams while solutions provided by other agencies are shown at the bottom of the plot. Solid lines represent observed displacement waveforms and dotted lines are the corresponding synthetics (all amplitudes are in cm, z: vertical, r: radial, t: transverse component).

▲ **Figure 4.** Moment tensor inversion results for the event that occurred on 11 December 2004 in mainland Greece. All symbols are the same as in Figure 3.

▲ **Figure 5.** Moment tensor inversion results for the event that occurred on 26 August 2005 in the area offshore Kefalonia island. All symbols are the same as in Figure 3.

network. This event was located in the area offshore Kefalonia island, Ionian Sea, at a depth of 14 km with local magnitudes M_{LATH} = 4.0 and M_{LAUT} = 3.5. The azimuthal coverage is not optimal, but we managed to cover approximately 180 degrees on the focal sphere by using four stations on the Greek mainland and Peloponnese (Figure 5). The misfit versus depth curve shows a plateau of minimum values (at 13, 15, 17 km) rather than one sharp minimum. The CLVD versus depth curve, on the other hand, exhibits a local minimum at 20 km; therefore we opt for a compromise between the two curves and select the solution at 17 km as the final one. No other agency has published a solution for this event since its signal-to-noise ratio is probably very low for stations at distances larger than 300 km. Its moment magnitude is equal to 3.7, which is closer to the automatically calculated local magnitude rather than M_{LATH}. This case highlights the difficulty of correctly calculating M_{LATH} for such small events originating at large distances from station ATH. It is obvious that in such cases the local magnitude will probably be overestimated.
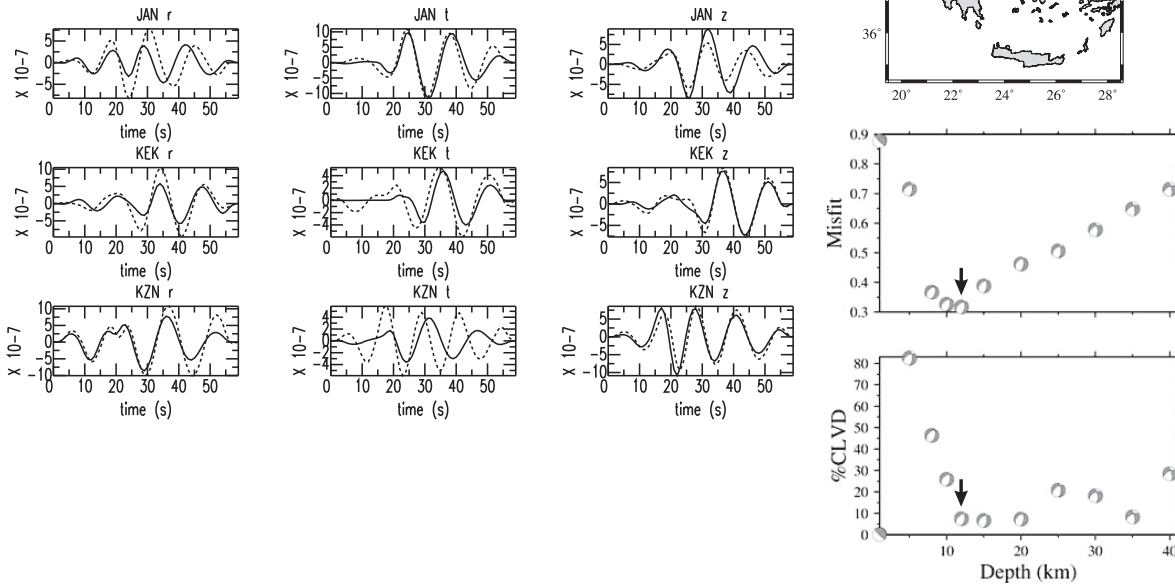
25 April 2002 07:28:08

Several earthquakes recorded by our network actually occur outside the political boundaries of Greece (mostly in southern Albania or western Turkey) but may be large enough to attempt a moment tensor inversion. The difficulties involved in such an attempt are obviously an inaccurate event location, limited azimuthal coverage (available stations only on the Greek side), and possible inadequacy of the velocity model. The example presented here is such a case; however, we managed to derive a reliable moment tensor despite these problems.
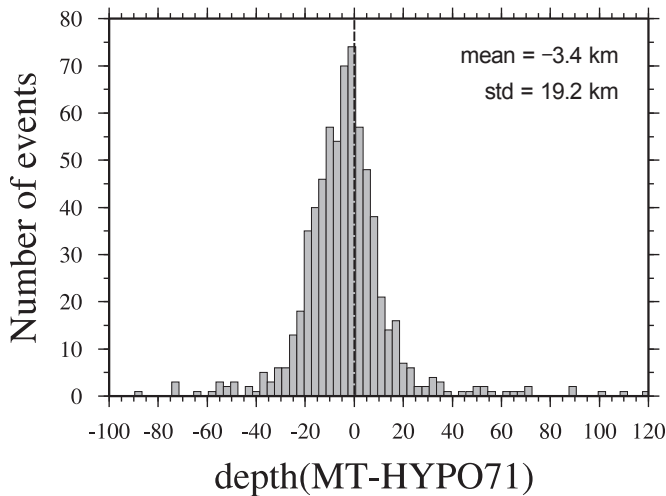
The event occurred on the Albanian side of the borders, near the Prespes Lakes, and was located by NOA at 9 km depth and with M_{LATH} = 4.2. Only three stations in our network were close enough to the epicenter, covering an azimuth of about 90 degrees on the focal sphere (Figure 6). We use the velocity model of Haslinger *et al.* (1999) for Green's functions calculations that we routinely utilize for events occurring in western Greece. The inversion results seem quite good though, with a sharp minimum of the misfit versus depth curve and a plateau for the CLVD versus depth. Again we opt for a compromise between the two curves and select the solution at 12 km as the final one. The fit between observed and synthetic waveforms is good and implies that the results are reliable, a suggestion that is confirmed by the NW-SE extension observed in this area (see Figure 1). The moment magnitude is equal to 4.0, which is quite close to the local magnitude estimate.

COMPARISON WITH NOA DEPTH AND LOCAL MAGNITUDES

In this section we compare the depth and moment magnitude derived from moment tensor inversion with the hypocentral depth and local magnitude of each event taken from the NOA catalog (available at http://www.gein.noa.gr/services/info-en.html). Figure 7 shows the distribution of the difference of the two depth values (depth MT – depth HYPO71) for all our events. The shape is approximately bell-shaped with its peak slightly shifted toward negative values as shown by a mean of -3.4 km, while the standard deviation is 19.2 km. This indicates that for more than half of our events the depth derived

▲ **Figure 6.** Moment tensor inversion results for the event that occurred on 25 April 2002 near the Greek-Albanian borders. All symbols are the same as in Figure 3.
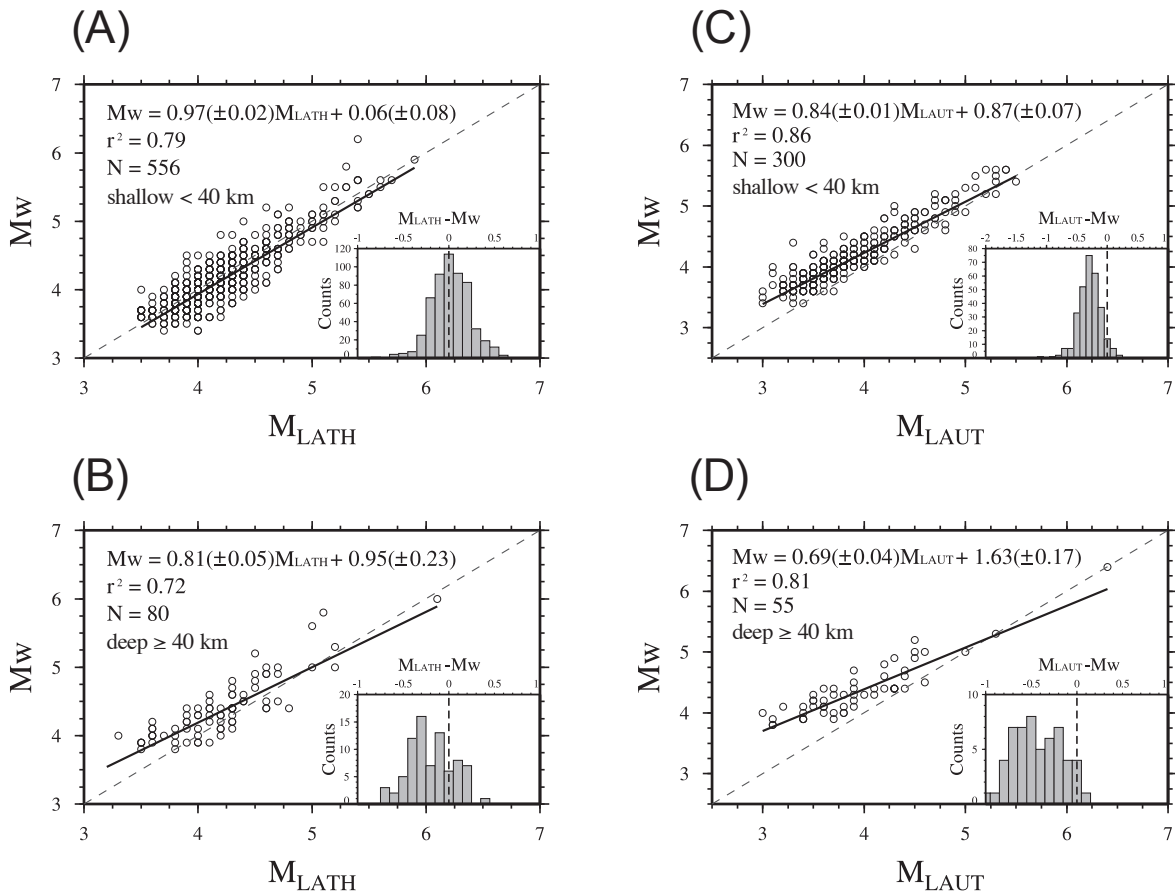

▲ **Figure 7.** Histogram showing the distribution of the difference between moment tensor minimum misfit/CLVD depth and HYPO71 hypocentral depth for 684 events that were inverted.

from moment tensor inversion is shallower than the HYPO71 depth. Hypocenters are difficult to constrain in cases when there is no recording station at distances of about 1.5 times the focal depth (Gomberg *et al.* 1990). This means that the shallower the event, the closer a station should be to the epicenter in order to obtain a reliable hypocentral depth. We speculate that the trend we observe here is due to the fact that during the period of our study the Hellenic network (HL) was quite sparse (station spacing 100 km or more); therefore there was

no station close enough to many of the shallow events we have modeled. Based on these arguments we consider that the depth derived from moment tensor inversion is more constrained than that from HYPO71 for events where no close station exists, or when the location is outside the NOA network.

Next we obtain a relationship between moment magnitude Mw and M_{LATH} through linear least-squares regression. Two things should be noted here: 1) a number of events that were inverted did not have a local magnitude value in the NOA catalog, thus only 636 events were finally used; and 2) the largest event that occurred during the interval of our study, the 8 January 2006 Kythira earthquake (Mw 6.7), had no calculated M_{LATH} value since the Wood-Anderson record was saturated. We separate our dataset into one part that consists of events originating shallower than 40 km and another for earthquakes with focal depths of 40 km or more. The two magnitude scales should show a close correspondence for shallow earthquakes, while larger differences are expected for deep events as suggested by previous studies (see Risteau 2009 and references therein). This is indeed what we observe in Figures 8A and B, where the distribution of the magnitudes difference (M_{LATH} − Mw) for shallow events has a mean value of 0.02 and a standard deviation of 0.2. The regression line also shows that the manually determined local magnitude is very close to the moment magnitudes we have estimated. For the deeper events the difference distribution is asymmetric and for most cases it is negative, implying that M_{LATH} is underestimated (sometimes by more than 0.5 units) with respect to moment magnitude.

A similar comparison and regression between Mw and M_{LAUT} after the year 2004 can be performed for shallow and

(A)

$Mw = 0.97(\pm0.02)M_{LATH} + 0.06(\pm0.08)$
$r^2 = 0.79$
$N = 556$
shallow < 40 km

$M_{LATH} - Mw$

Counts

M_{LATH}

(C)

$Mw = 0.84(\pm0.01)M_{LAUT} + 0.87(\pm0.07)$
$r^2 = 0.86$
$N = 300$
shallow < 40 km

$M_{LAUT} - Mw$

Counts

M_{LAUT}

(B)

$Mw = 0.81(\pm0.05)M_{LATH} + 0.95(\pm0.23)$
$r^2 = 0.72$
$N = 80$
deep ≥ 40 km

$M_{LATH} - Mw$

Counts

M_{LATH}

(D)

$Mw = 0.69(\pm0.04)M_{LAUT} + 1.63(\pm0.17)$
$r^2 = 0.81$
$N = 55$
deep ≥ 40 km

$M_{LAUT} - Mw$

Counts

M_{LAUT}

▲ **Figure 8.** A) Diagram showing the regression results between *Mw* and local magnitude calculated using the analog Wood-Anderson records at station ATH for shallow events; B) the same for deeper events. C) Diagram showing the regression results between *Mw* and automatic local magnitude calculated using synthetic Wood-Anderson traces following the procedure of Hutton and Boore (1987) for shallow events; D) the same for deeper events. In all the plots the solid line represents the least-squares fit and the dashed one the line with slope 1.0, N is the total number of events used in each regression (see text for more details), and r^2 is the correlation coefficient. The insets show the distribution of the difference between local and moment magnitudes in each case and the dotted line signifies the 0.0 difference of the two magnitudes.
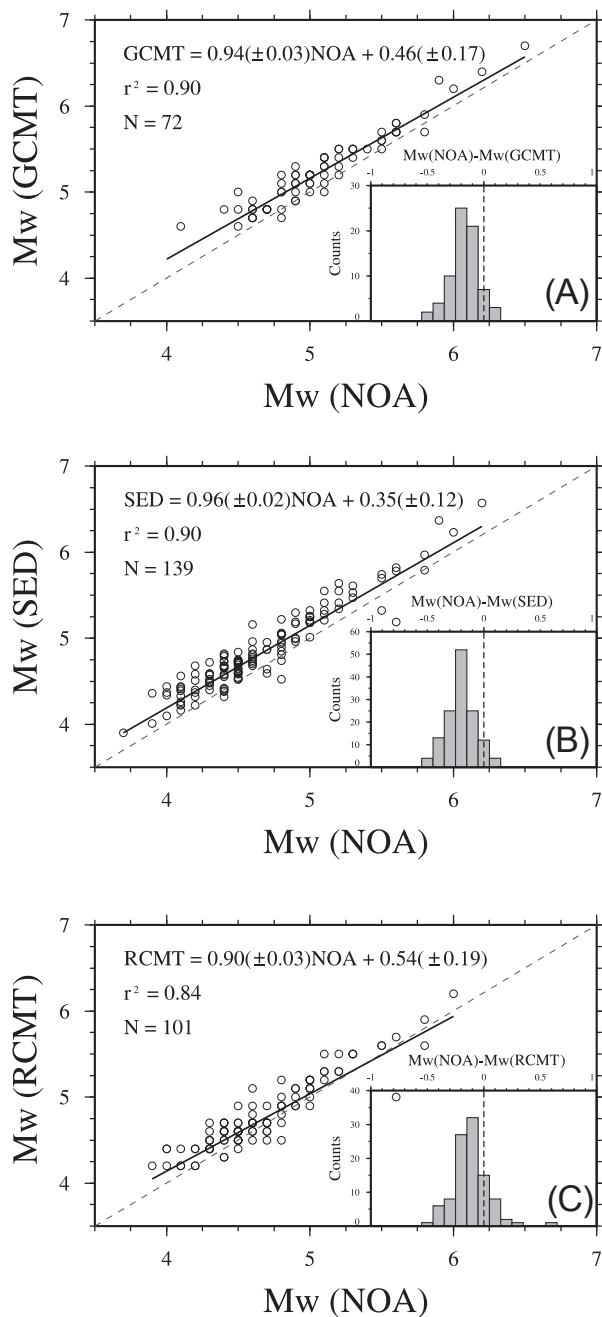
deep events (Figures 8C and D). For the case of shallow earthquakes we observe a high linear correlation coefficient and a regression line that progressively coincides with $Mw = M_{LAUT}$ for local magnitudes larger than about 4.5. This result stresses the importance of the automatic determination of M_L as a fast and reliable estimate of event magnitude that can help trigger a quick response from government agencies in the case of large earthquakes. However, in most cases M_{LAUT} is smaller than the corresponding moment magnitude while this underestimation trend becomes more significant for earthquakes deeper than 40 km.

COMPARISON WITH OTHER MOMENT TENSOR DATABASES

First we compare our moment magnitude estimates with those for manually reviewed solutions from GCMT, SED, and RCMT groups, respectively (Figure 9). As expected, the number of common events between our database and the others is smaller (N = 72) for the teleseismically determined
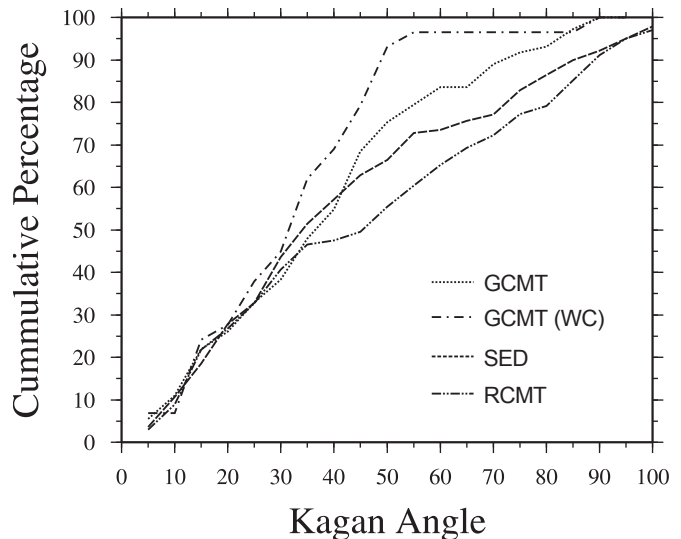
dataset (GCMT) and larger (N = 139, N = 101) for the regional moment tensor databases (SED, RCMT, respectively). However, the lowest moment magnitude of these common events is around 4.0 for all three databases. The comparison of moment magnitudes reveals high values of correlation coefficients (0.84–0.90), which signifies that our *Mw* estimates are compatible with those issued by other agencies. Histograms of the differences between NOA-determined *Mw* and other *Mw* estimates show that in all three cases our *Mw* is underestimated on average by 0.11–0.19 magnitude units. This underestimation of moment magnitude can be explained in terms of the limited bandwidth of our instruments, which can record periods only up to 20 s, contrary to the other three agencies where the used bandwidth is significantly broader (20–135 s).

We also check the correspondence between the focal mechanisms derived by NOA and the other three databases by using as a measure of similarity the Kagan angle (Kagan 1991). In the case of GCMT we perform this comparison first for all 72 common events and then for a subset of well-determined GCMT moment tensors. This well-determined subset follows

▲ **Figure 10.** Cumulative percentage of Kagan angles for all common pairs of events between NOA and GCMT, SED, RCMT moment tensor databases. GCMT(WC) represents well-constrained Global CMT solutions that pass the criteria set by Frohlich and Davies (1999) (see text for more details).

▲ **Figure 9.** A) Diagram showing regression results between *Mw*(GCMT) and *Mw*(NOA). Symbols are the same as in Figure 8. The inset shows a histogram of the distribution of differences between moment magnitudes of GCMT and NOA. The dotted line signifies the 0.0 difference of the two magnitudes. B) Same as in (A) for *Mw*(SED) and *Mw*(NOA); C) Same as in (A) for *Mw*(RCMT) and *Mw*(NOA).

the criteria suggested by Frohlich and Davies (1999), where the relative error of the moment tensor elements should be less than 0.5, the CLVD component less than 20%, and no moment tensor element is fixed during the inversion. Results indicate that for the entire dataset, about 50% of common event pairs have Kagan angles smaller than 35 degrees (Figure 10). This percentage becomes 62% if we consider only the well-determined

GCMT moment tensors. The situation is similar for the SED and RCMT, with 52% and 47% of common pairs, respectively, with Kagan angles less than 35 degrees.

CONCLUDING REMARKS

The main conclusions after the analysis of this sizable moment tensor database can be summarized as follows:

We successfully inverted 684 events in the moment magnitude range 3.6–6.7 that occurred either within the political boundaries of Greece, or in the surrounding regions using data recorded by the Hellenic seismic (HL) network operated by NOA.

For more than half of our events the depth obtained by moment tensor inversion is shallower than its equivalent reported by routine location using travel times. This can probably be explained by the fact that in the interval 2001–2006 the HL network was quite sparse, so there were few stations close to the epicenter to record *P* and *S* phases.

Linear regressions of moment magnitude versus manual and automatic local magnitudes calculated by NOA show high correlation coefficients for events originating at shallow (< 40 km) depths. A close correspondence between moment and local magnitude within 0.2 units on average can be observed, supporting previous findings that were based on a much smaller number of events (Melis and Konstantinou 2006). As expected this correspondence is less pronounced for deeper earthquakes where local magnitude estimates are underestimated with respect to moment magnitude.

A comparison of moment magnitudes calculated in this study with those routinely reported by other agencies (GCMT, SED, RCMT) shows correlation coefficients between 0.84– 0.90 and a mean difference of 0.1–0.2 units, confirming the

robustness of our magnitude estimates. Common pairs of moment tensor solutions are also similar to a percentage that varies between 62%–47% depending on which database is used for comparison.

This study focused on moment tensor solutions only for the years 2001–2006; however, a wealth of waveform data have accumulated after this period and efforts are underway to invert more events. The unification of the HL network with the other three regional networks mentioned earlier has increased the total number of available stations and the coverage in very active areas such as the northern Aegean, the Corinth Gulf, and western Greece. This means that initial locations can be more accurate and there is also greater choice in selecting stations for inversion at different azimuths. Improvement of the existing 1-D velocity models for Green's functions calculations is perhaps the next necessary step that must be taken toward reliable, near real-time determination of moment tensors in the Greek region.

ACKNOWLEDGMENTS

REFERENCES

Baker, C., D. Hatzfeld, H. Lyon-Caen, E. Papadimitriou, and A. Rigo (1997). Earthquake mechanisms of the Adriatic Sea and western Greece: Implications for the oceanic subduction-continental collision transition. *Geophysical Journal International* **131**, 559–594.

Benetatos, C., A. Kiratzi, C. Papazachos, and G. Karakaisis (2004). Focal mechanisms of shallow and intermediate depth earthquakes along the Hellenic arc. *Journal of Geodynamics* **37**, 253–296; doi:10.1016/j.jog.2004.02.002.

Benetatos, C., A. Kiratzi, Z. Roumelioti, G. Stavrakakis, G. Drakatos, and I. Latoussakis (2005). The 14 August 2003 Lefkada island (Greece) earthquake: Focal mechanisms of the mainshock and of the aftershock sequence. *Journal of Seismology* **9**, 171–190; doi:10.1007/s10950-005-7092-1.

Bernard, P., P. Briole, B. Meyer, H. Lyon-Caen, J. M. Gomez, C. Tiberi, C. Berge *et al.* (1997). The *Ms* = 6.2, June 15 1995 Aigion earthquake (Greece): Evidence for low angle normal faulting in the Corinth rift. *Journal of Seismology* **1**, 131–150.

Braunmiller, J., U. Kradolfer, M. Baer, and D. Giardini (2002). Regional moment tensor determination in the European-Mediterranean area—initial results. *Tectonophysics* **356**, 5–22.

Clinton, J. F., E. Hauksson, and K. Solanki (2006). An evaluation of the SCSN moment tensor solutions: Robustness of the *Mw* magnitude scale, style of faulting and automation of the method. *Bulletin of the Seismological Society of America* **96**, 1,689–1,705; doi:10.1785/0120050241.

Engdahl, E. R., R. D. van der Hilst, and R. P. Buland (1998). Global teleseismic earthquake relocation with improved travel time and procedures for depth determination. *Bulletin of the Seismological Society of America* **88**, 722–743.

Evangelidis, C., K. I. Konstantinou, N. S. Melis, M. Charalambakis, and G. N. Stavrakakis (2008). Waveform relocation and focal mechanism analysis of an earthquake swarm in Trichonis Lake, western Greece. *Bulletin of the Seismological Society of America* **98**, 804–811; doi:10.1785/0120070185.

Frohlich, C., and S. D. Davis (1999). How well are well-constrained *T*, *B* and *P* axes in moment tensor catalogs? *Journal of Geophysical Research* **104**, 4,901–4,910.

Ghose, S., M. W. Hamburger, and C. J. Ammon (1998). Source parameters of moderate-sized earthquakes in the Tien-Shan, central Asia from regional moment tensor inversion. *Geophysical Research Letters* **25**, 3,181–3,184.

Gomberg, J. S., K. M. Shedlock, and S. W. Roecker (1990). The effect of *S*-wave arrival times on the accuracy of hypocentre estimation. *Bulletin of the Seismological Society of America* **80**, 1,605–1,628.

Hatzfeld, D., D. Kementzetzidou, V. Karakostas, M. Ziazia, S. Nothard, D. Diagourtas, A. Deschamps *et al.*, (1996). The Galaxidi earthquake of 18 November 1992: A possible asperity within the normal fault system of the Gulf of Corinth (Greece). *Bulletin of the Seismological Society of America* **86**, 1,987–1,991.

Haslinger, F., E. Kissling, J. Ansorge, D. Hatzfeld, E. Papadimitriou, V. Karakostas, K. Makropoulos, H.-G. Kahle, and Y. Peter (1999). 3D crustal structure from local earthquake tomography around the Gulf of Arta (Ionian region, NW Greece). *Tectonophysics* **304**, 201–218.

Hollenstein, C., M. D. Müller, A. Geiger, and H.-G. Kahle (2008). Crustal motion and deformation in Greece from a decade of GPS measurements, 1993–2003. *Tectonophysics* **449**, 17–40; doi:10.1016/j.tecto.2007.12.006

Hutton, L. K., and D. M. Boore (1987). The *ML* scale in southern California. *Bulletin of the Seismological Society of America* **77**, 2,074–2,094.

Kagan, Y. Y. (1991). 3-D rotation of double-couple earthquake sources. *Geophysical Journal International* **106**, 709–716.

Kao, H., and P. R. Jian (2001). Seismogenic patterns in the Taiwan region: Insights from source parameter inversion of BATS data. *Tectonophysics* **333**, 179–198.

Karagianni, E. E., C. B. Papazachos, D. G. Panagiotopoulos, P. Suhaldoc, A. Vuan, and G. F. Panza (2005). Shear velocity structure in the Aegean area obtained by inversion of Rayleigh waves. *Geophysical Journal International* **160**, 127–143; doi:10.1111/j.1365-246X.2005.02354.x.

Kennett, B. N. L. (1983). *Seismic Wave Propagation in Stratified Media*. Cambridge: Cambridge University Press.

Kiratzi, A., and E. Louvari (2003). Focal mechanisms of shallow earthquakes in the Aegean Sea and the surrounding lands determined by waveform modelling: A new database. *Journal of Geodynamics* **36**, 251–274; doi:10.1016/S0264-3707(03)00050-4.

Konstantinou, K. I., I. S. Kalogeras, N. S. Melis, M. C. Kourouzidis, and G. N. Stavrakakis (2006). The 8 January 2006 earthquake (*Mw* 6.7) offshore Kythira island, southern Greece: Seismological, strong-motion and macroseismic observations of an intermediate-depth event. *Seismological Research Letters* **77**, 544–553.

Konstantinou, K. I., S.-J. Lee, C. P. Evangelidis, and N. S. Melis (2009). Source process and tectonic implications of the 8 January 2006 (*Mw* 6.7) Kythira earthquake, southern Greece. *Physics of the Earth and Planetary Interiors* **175**, 167–182; doi:10.1016/j.pepi.2009.03.010.

Konstantinou, K. I., N. S. Melis, S.-J. Lee, C. P. Evangelidis, and K. Boukouras (2009). Rupture process and aftershocks relocation of the 8 June 2008 *Mw* 6.4 NW Peloponnese, Western Greece. *Bulletin of the Seismological Society of America* **99**, 3,374–3,389; doi:10.1785/0120080301.

Kubo, A., E. Fukuyama, H. Kawai, and K. Nonomura (2002). NEID seismic moment tensor catalogue for regional earthquakes around Japan: Quality test and application. *Tectonophysics* **356**, 23–48.

Lee, W. H. K., and J. C. Lahr (1972). *HYPO71: A Computer Program for Determining Hypocenter, Magnitude and First Motion Pattern for Local Earthquakes*. USGS Open-File Report, 100 pp.

Le Pichon, X., and J. Angelier (1979). The Hellenic arc and trench system: A key to the neotectonic evolution of the eastern Mediterranean area. *Tectonophysics* **60**, 1–42.

Le Pichon, X., N. Chamot-Rooke, S. Lallemant, R. Noomen, and G. Veis (1995). Geodetic determination of the kinematics of central Greece with respect to Europe: Implications for eastern Mediterranean tectonics. *Journal of Geophysical Research* **100**, 12,675–12,690.

Lyon-Caen, H., R. Armijo, J. Drakopoulos, J. Baskoutas, N. Delibasis, R. Gaulon, V. Kouskouna *et al.*, (1988). The 1986 Kalamata (south Peloponnese) earthquake: Detailed study of a normal fault, evidence for an east-west extension in the Hellenic arc. *Journal of Geophysical Research* **93**, 14,967–15,000.

McClusky S., S. Balassanian, A. Barka, C. Demir, S. Ergintav, I. Georgiev, O. Gurkan *et al.*, (2000). Global positioning system constraints on plate kinematics and dynamics in the eastern Mediterranean and Caucasus. *Journal of Geophysical Research* **105**, 5,695–5,719.

Melis, N. S., G. N. Stavrakakis, and J. Zahradnik (2001). Focal properties of the $Mw = 6.5$ Skyros, Aegean Sea, earthquake. *ORFEUS Electronic Newsletter* **3** (2), 11.

Melis, N. S., and K. I. Konstantinou (2006). Real-time seismic monitoring in the Greek region: An example from the 17 October 2005 east Aegean Sea earthquake sequence. *Seismological Research Letters* **77**, 364–370.

Novotny, O., J. Zahradnik, and G. A. Tselentis (2001). Northwestern Turkey earthquakes and the crustal structure inferred from surface waves observed in western Greece. *Bulletin of the Seismological Society of America* **91**, 875–879.

Papadopoulos, G. A., D. Kondopoulou, G.-A. Leventakis, and S. Pavlides (1986). Seismotectonics of the Aegean region. *Tectonophysics* **124**, 67–84.

Papazachos, B. C., V. G. Karakostas, C. B. Papazachos, and E. M. Scordilis (2000). The geometry of the Wadati-Benioff zone and lithospheric kinematics in the Hellenic arc. *Tectonophysics* **319**, 275–300.

Papazachos, B., A. Kiratzi, B. Karakostas, D. Panagiotopoulos, E. Scordilis, and D. M. Mountrakis (1988). Surface fault traces, fault plane solutions and spatial distribution of the aftershocks of the September 13, 1986 earthquake of Kalamata (southern Greece). *Pure and Applied Geophysics* **126**, 55–68.

Papazachos, C. B., and G. Nolet (1997). *P* and *S* velocity structure of the Hellenic area obtained by robust nonlinear inversion of travel times. *Journal of Geophysical Research* **102**, 8,349–8,367.

Papazachos, B. C., D. G. Panagiotopoulos, T. M. Tsapanos, D. M. Mountrakis, and G. C. Dimopoulos (1983). A study of the 1980 summer seismic sequence in the Magnesia region of central Greece. *Geophysical Journal of the Royal Astronomical Society* **75**, 155–168.

Papazachos, B. C., and K. Papazachou (1997). *The Earthquakes of Greece*. Thessaloniki, Greece: Ziti Editions.

Pondrelli, S., A. Morelli, G. Ekström, S. Mazza, E. Boschi, and A. M. Dziewonski (2002). European-Mediterranean regional centroid-moment tensors: 1997–2000. *Physics of the Earth and Planetary Interiors* **130**, 71–101.

Randall, G. E. (1994). Efficient calculation of complete differential seismograms for laterally homogeneous earth models. *Geophysical Journal International* **118**, 245–254.

Randall, G. E., C. J. Ammon, and T. J. Owens (1995). Moment tensor estimation using regional seismograms from a Tibetan plateau portable network deployment. *Geophysical Research Letters* **22**, 1,665–1,668.

Richter, C. F. (1935). An instrumental earthquake magnitude scale. *Bulletin of the Seismological Society of America* **25**, 1–32.

Risteau, J. (2008). Implementation of routine regional moment tensor analysis in New Zealand. *Seismological Research Letters* **79**, 400–415; doi:10.1785/gssrl.81.5.400.

Risteau, J. (2009). Comparison of magnitude estimates for New Zealand earthquakes: Moment magnitude, local magnitude and teleseismic body-wave magnitude. *Bulletin of the Seismological Society of America* **99**, 1,841–1,852; doi:10.1785/0120080237.

Ritsema, J., and T. Lay (1995). Long-period regional wave moment tensor inversion for earthquakes in the western United States. *Journal of Geophysical Research* **100**, 9,853–9,864.

Roumelioti, Z., C. Benetatos, A. Kiratzi, G. Stavrakakis, and N. Melis (2004). A study of the 2 December 2002 (**M** 5.5) Vartholomio (western Peloponnese, Greece) earthquake and of its largest aftershocks. *Tectonophysics* **387**, 65–79; doi:10.1016/j.tecto.2004.06.008.

Sachpazi, M., A. Hirn, C. Clément, F. Haslinger, M. Laigle, E. Kissling, P. Charvis, Y. Hello, J.-C. Lépine, M. Sapine, and J. Ansorge (2000). Western Hellenic subduction and Cephalonia transform: Local earthquakes and plate transport and strain. *Tectonophysics* **319**, 301–319.

Stich, D., C. J. Ammon, and J. Morales (2003). Moment tensor solutions for small and moderate earthquakes in the Ibero-Maghreb region. *Journal of Geophysical Research* **108**, 2,148; doi:10.1029/2002JB002057.

Thio, H. K., and H. Kanamori (1996). Source complexity of the 1994 Northridge earthquake and its relation to aftershock mechanisms. *Bulletin of the Seismological Society of America* **86**, S84–S92.

Zhao, L. S., and D. V. Helmberger (1994). Source estimation from broadband regional seismograms. *Bulletin of the Seismological Society of America* **84**, 91–104.

Institute of Geophysics
National Central University
Jhongli, 320 Taiwan
kkonst@ncu.edu.tw
(K. I. K.)